Along-the-path exponential integration for Floquet stability analysis of wind turbines

To cite this article: J Ros *et al* 2022 *J. Phys.: Conf. Ser.* **2265** 032026

Along-the-path exponential integration for Floquet stability analysis of wind turbines

J Ros[1,2], A Olcoz[2] and A Plaza[2]

[1] Institute of Smart Cities (ISC), Public University of Navarre (UPNA), Campus of Arrosadia, 31006 Pamplona, Spain
[2] Engineering Department, Public University of Navarre (UPNA), Campus of Arrosadia, 31006 Pamplona, Spain

E-mail: [jros, alvaro.olcoz, aitor.plaza]@unavarra.es

Abstract. Traditionally, stability assessment of wind turbines has been performed by eigenanalysis of the azimuthally-averaged linearized system after applying the Multi-Blade Coordinate (MBC) transformation. However, due to internal or external anisotropy, the MBC transform does not produce an exact Linear Time-Invariant (LTI) system, and a Floquet analysis is required to capture the influence of all periodic terms, leading to a more accurate stability analysis. In this paper exponential integration methods that use system linearizations at different blade azimuth positions are used to integrate the perturbed system state and compute the Floquet monodromy matrix. The proposed procedure is assessed for a simple 6 DOF wind turbine model and a more complex aeroelastic model of a 5MW onshore wind turbine. The defined *along-the-path* or *moving-point* exponential integrator is found to be the suitable in order to perform a Floquet stability analysis even using a coarse linearization grid.

1. Introduction

An important aspect of the dynamic response of wind turbines is the potential presence of instabilities or critically low-damped modes. Current tools for stability and modal analysis of wind turbines can be classified as linear and non-linear (OMA, POMA, PARMAX...) [1]. Our work falls within the scope of the linear ones.

Coleman [2] introduced a transformation of physical blade coordinates into multi-blade coordinates (MBC) describing the rotor motion as a whole in the inertial or fixed reference frame. For rotors with three or more isotropic blades, the Coleman or MBC transformation provides a means to model an intrinsically periodic system such as a wind turbine so it closely resembles Linear Time-Invariant (LTI) one, allowing the use of well-known LTI modal analysis and control techniques. Hansen [3] used the MBC transformation to improve modal dynamics in order to avoid stall-induced edgewise vibrations and later combined it with an eigenvalue approach to obtain modal properties of a three-bladed wind turbine model [4]. Bir [5, 6] used MBC in conjunction with the aeroelastic code FAST [7] to study stability and modal characteristics of a 5 MW wind turbine and later implemented the MATLAB code MBC3.

For a Linear Time-Periodic (LTP) system, the MBC transformation does not produce an exact LTI model. Interestingly, it filters out the periodic terms in the equations of motion except the integral multiples of ΩN_b, where Ω is the rotor speed and N_b is the number of blades [5]. The MBC transformation only renders the system LTI when the system is internally

(identical and symmetrically mounted blades) and externally (absence of tower shadow, wind shear and gravity) isotropic. As system isotropy is difficult to asses and quantify *a priori*, a Floquet analysis should be preferred to perform a strict stability and modal analysis of the wind turbine [5, 8].

In the context of wind turbines, Stol and Balas [9] used classical Floquet analysis to study the modal behaviour of a 2-bladed teetered rotor wind turbine for different DOF models. Later, Stol [10] compared the results of using the MBC transformation and Floquet analysis to study the modal parameters of the 5 MW NREL onshore wind turbine, finding only significant differences for the idling extreme operation DLC of the IEC standard. Skjoldan and Hansen [11, 12] showed the similarity between Coleman and Lyapunov-Floquet (L-F) transformations, being the former a special case of the L-F transformation when the rotor is internally and externally isotropic. Skjoldan [11, 13] also used Floquet theory to show how blade anisotropy creates additional harmonic terms in the solutions, and Tcherniak [14] proposed mode shape asymmetry of an anisotropic rotor as a blade damage indicator. Following the approach of Peters et *al.* [15], Bottasso and Cacciola [8] used Floquet theory and modal participation factors to analyze the harmonics present in the response of a simple edgewise hinged blade model, including tower side-side motion. They revealed infinite number of harmonics, with the most noticeable ones around the frequency spectrum of the response.

Classical Floquet analysis requires the computation of the state transition matrix over a period by integrating the system for a set of linearly independent initial conditions perturbing the steady periodic trajectory. Ros et *al.* [16] showed that even if exponential integrators are rare in multibody dynamics literature, they exhibit outstanding characteristics, demonstrating it for a simple, rigid and flexible nonlinear mechanical systems.

In this paper innovative exponential integration methods of the perturbed system state are proposed. These are based on a set of system linearizations at different blade azimuth positions. They are used to compute the Floquet monodromy matrix, whose eigenvalues rule the stability of the system. These exponential integration methods are assessed for integration and Floquet stability analysis for a simple 6 DOF model and the well-known 5 MW NREL onshore aeroelastic wind turbine model using the OpenFAST linearization capability. In this model, the effect of adding rotor internal anisotropy is also assessed.

2. Stability and modal analysis of wind turbines

A general first order linear differential equation can be expressed as:

$$\dot{\mathbf{x}}(t) = \mathbf{A}(t)\mathbf{x}(t) + \mathbf{B}(t)\mathbf{u}(t), \tag{1}$$

where $\mathbf{x}(t)$ and $\mathbf{u}(t)$ are the state and input vectors, respectively, and $\mathbf{A}(t)$ and $\mathbf{B}(t)$ are the system state and input matrices. For a T-periodic linear dynamic system, the system and input matrices are periodic, $\mathbf{A}(t+T) = \mathbf{A}(t)$ and $\mathbf{B}(t+T) = \mathbf{B}(t)$. Let the second order LTP dynamical system

$$\mathbf{M}(t)\ddot{\mathbf{q}}(t) + \mathbf{C}(t)\dot{\mathbf{q}}(t) + \mathbf{K}(t)\mathbf{q}(t) = 0, \tag{2}$$

where $\mathbf{q}(t)$ is the vector of generalized coordinates and $\mathbf{M}(t) = \mathbf{M}(t+T)$, $\mathbf{C}(t) = \mathbf{C}(t+T)$, $\mathbf{K}(t) = \mathbf{K}(t+T)$, are the mass, damping and stiffness matrices, respectively. Defining $\mathbf{x} = [\mathbf{q}^\top, \dot{\mathbf{q}}^\top]^\top$, this system system can be cast into first order form given by (1). Then, the system state matrix becomes

$$\mathbf{A}(t) = \begin{bmatrix} \mathbf{0} & \mathbf{1} \\ -\mathbf{M}(t)^{-1}\mathbf{K}(t) & -\mathbf{M}(t)^{-1}\mathbf{C}(t) \end{bmatrix}. \tag{3}$$

2.1. Coleman transformation

For an internally (identical and symmetrically mounted blades) and externally (absence of tower shadow, wind shear and gravity) isotropic system, the Coleman or Multi-Blade Coordinate (MBC) transformation [2] for bladed rotors renders the system LTI. Then, stability and modal analysis can be performed by simple eigenanalysis of the transformed system matrix.

Let $\left[q_1^j, q_2^j, q_3^j\right]^\top$ be the blade coordinates in the rotating frame corresponding to the jth degree of freedom (DOF) of a 3-bladed rotor. The MBC-transformed coordinates $\left[a_0^j, a_1^j, b_1^j\right]^\top$ are defined through the following relation:

$$\begin{bmatrix} q_1^j(t) \\ q_2^j(t) \\ q_3^j(t) \end{bmatrix} = \tilde{\mathbf{t}}(t) \begin{bmatrix} a_0^j(t) \\ a_1^j(t) \\ b_1^j(t) \end{bmatrix} = \begin{bmatrix} 1 & \cos\psi_1(t) & \sin\psi_1(t) \\ 1 & \cos\psi_2(t) & \sin\psi_2(t) \\ 1 & \cos\psi_3(t) & \sin\psi_3(t) \end{bmatrix} \begin{bmatrix} a_0^j(t) \\ a_1^j(t) \\ b_1^j(t) \end{bmatrix}, \tag{4}$$

where $\psi_i = \Omega t + \frac{2}{3}\pi(i-1)$ is the azimuth angle of blade number i and $\Omega = 2\pi/T$ is the mean rotational speed of the rotor. The physical interpretation of the transformed coordinates can be found in [3–6].

The full state vector $\mathbf{x}(t) = [\mathbf{q}(t)^\top, \dot{\mathbf{q}}(t)^\top]^\top$ of a generic wind turbine system containing DOFs in the rotating and fixed reference frames can be expressed in multi-blade coordinates $\mathbf{z}_C(t)$ using the following transformation:

$$\mathbf{x}(t) = \mathbf{T}_C(t)\mathbf{z}_C(t), \tag{5}$$

where

$$\mathbf{T}_C(t) = \begin{bmatrix} \begin{bmatrix} \mathbf{I}_{N_f} & & & \\ & \tilde{\mathbf{t}}(t) & & \\ & & \ddots & \\ & & & \tilde{\mathbf{t}}(t) \end{bmatrix}_{N_q} & \mathbf{0}_{N_q} \\ \frac{d}{dt}\begin{bmatrix} \mathbf{I}_{N_f} & & & \\ & \tilde{\mathbf{t}}(t) & & \\ & & \ddots & \\ & & & \tilde{\mathbf{t}}(t) \end{bmatrix}_{N_q} & \begin{bmatrix} \mathbf{I}_{N_f} & & & \\ & \tilde{\mathbf{t}}(t) & & \\ & & \ddots & \\ & & & \tilde{\mathbf{t}}(t) \end{bmatrix}_{N_q} \end{bmatrix}_{N_s}. \tag{6}$$

N_f is the number of DOFs in the fixed reference frame, N_q the total number of DOFs of the system, and $N_s = 2N_q$ the number of elements in the state vector. By substitution of (5) into system equation (1), the MBC-transformed system equation $\dot{\mathbf{z}}_C(t) = \mathbf{A}_C(t)\mathbf{z}_C(t) + \mathbf{B}_C(t)\mathbf{u}_C(t)$ is obtained, where

$$\mathbf{A}_C(t) = \mathbf{T}_C^{-1}(t)\left(\mathbf{A}(t)\mathbf{T}_C(t) - \dot{\mathbf{T}}_C(t)\right) \tag{7}$$

is the transformed system matrix, which will be time-invariant if the above mentioned isotropicity conditions are fulfilled. For systems with isotropic blades under moderate wind shear conditions in normal operation, the transformed system matrix is closely time-invariant, and aeroelastic modal properties are usually calculated based on the eigenanalysis of the azimuthally-averaged system matrix.

However, for systems with higher degree of anisotropy, the Coleman transformation does not produce an exact LTI system. Still, it provides strong reduction on the periodic time dependency of the system matrix elements, leading to numerically well-conditioned system equations, which is highly desirable if a subsequent Floquet analysis is to be performed. In order to assess the stability of a generic LTP system it is necessary to introduce the so-called Lyapunov-Floquet (L-F) transformation [17, 18].

2.2. Lyapunov-Floquet transformation

A fundamental solution of the T-periodic system (1) consists of N solutions calculated by numerical integration over a period T with a linearly independent initial condition set. These solutions are arranged as columns of the so-called *fundamental solution matrix*:

$$\boldsymbol{\varphi}(t) = \left[\ \boldsymbol{\varphi}_1(t), \quad \boldsymbol{\varphi}_2(t), \quad \dots \quad , \boldsymbol{\varphi}_N(t) \ \right]. \tag{8}$$

Hence, $\dot{\boldsymbol{\varphi}}(t) = \mathbf{A}(t)\boldsymbol{\varphi}(t)$. Periodicity in $\mathbf{A}(t)$ means that $\boldsymbol{\varphi}(t+T)$ is a solution of the system, $\dot{\boldsymbol{\varphi}}(t+T) = \mathbf{A}(t)\boldsymbol{\varphi}(t+T)$, and $\boldsymbol{\varphi}(t+T)$ can be expressed as a linear combination of $\boldsymbol{\varphi}(t)$ as:

$$\boldsymbol{\varphi}(t_0+T) = \boldsymbol{\varphi}(t_0)\mathbf{C}, \tag{9}$$

where $\mathbf{C} = \boldsymbol{\varphi}^{-1}(t_0)\boldsymbol{\varphi}(t_0+T)$ is a non-singular matrix termed *monodromy matrix* of the system[1]. The eigenvalues $(\rho_1, \rho_2, ..., \rho_k)$ of the *monodromy matrix* known as *characteristic* or *Floquet multipliers* rule the stability of the periodic system. The system will be asymptotically stable if all the multipliers lie inside the open unit disk in the complex plane, $|\rho_k| < 1; \ \forall \ k$.

The main theorem of Floquet theory, Floquet's theorem [17], gives a canonical form for each fundamental matrix solution of system, which consists in a product of a purely periodic matrix and a matrix exponential:

$$\boldsymbol{\varphi}(t) = \mathbf{L}(t)\mathbf{L}^{-1}(t_0)\boldsymbol{\varphi}(t_0)\mathrm{e}^{\mathbf{R}(t-t_0)}, \tag{10}$$

where $\mathbf{R}$ is a constant non-singular matrix termed *Floquet factor*, $\boldsymbol{\varphi}(t)$ a fundamental solution matrix of the system, $\mathbf{L}(t)$ the T-periodic Lyapunov-Floquet (L-F) transformation and the terms $\mathbf{L}^{-1}(t_0)$ and $\boldsymbol{\varphi}(t_0)$ are introduced to make the transformation independent of the choice of initial conditions used to compute the fundamental solution matrix (8). Making $t = t_0 + T$ in (10) the relationship between the *monodromy matrix* $\mathbf{C}$ and the *Floquet factor* $\mathbf{R}$ is obtained:

$$\mathbf{C} = \boldsymbol{\varphi}^{-1}(t_0)\boldsymbol{\varphi}(t_0+T) = \mathrm{e}^{\mathbf{R}T}. \tag{11}$$

The L-F transformation [17,18] is the bounded, periodic and invertible transformation of the state vector defined as $\mathbf{x}(t) = \mathbf{L}(t)\mathbf{z}_{LF}(t)$. The L-F transformed LTI system is given by:

$$\dot{\mathbf{z}}_{LF}(t) = \mathbf{A}_{\mathrm{L}}\mathbf{z}_{LF}(t), \tag{12a}$$

$$\mathbf{A}_{\mathrm{L}} = \mathbf{L}^{-1}(t)(\mathbf{A}(t)\mathbf{L}(t) - \dot{\mathbf{L}}(t)). \tag{12b}$$

The transformed system matrix $\mathbf{A}_{\mathrm{L}}$ is proven to be time-invariant by substitution of $\mathbf{L}(t) = \boldsymbol{\varphi}(t)\mathrm{e}^{-R(t-t_0)}\boldsymbol{\varphi}^{-1}(t_0)\mathbf{L}(t_0)$ and its time derivative in (12b), yielding:

$$\mathbf{A}_{\mathrm{L}} = \mathbf{L}^{-1}(t_0)\boldsymbol{\varphi}(t_0)\mathbf{R}\boldsymbol{\varphi}^{-1}(t_0)\mathbf{L}(t_0). \tag{13}$$

Matrices $\mathbf{A}_{\mathrm{L}}$ and $\mathbf{R}$ have the same eigenvalues as they are similar, thus, either of them can be used to asses the stability and extract the modal properties of the continuous system.

Matrix $\mathbf{R}$ can be computed form the monodromy matrix $\mathbf{C}$ as:

$$\mathbf{R} = \frac{1}{T}\ln(\mathbf{C}). \tag{14}$$

In this way matrix $\mathbf{R}$ is undetermined due to the indeterminacy of the matrix logarithm. However, if matrix $\mathbf{C}$ is Jordan decomposed as $\mathbf{C} = \mathbf{P}\mathbf{J}\mathbf{P}^{-1}$ with Jordan form $\mathbf{J} = \mathrm{diag}\{\rho_1, \rho_2, \dots, \rho_N\}$, then in the Jordan decomposition $\mathbf{R} = \mathbf{V}\boldsymbol{\Lambda}\mathbf{V}^{-1}$, $\boldsymbol{\Lambda}$ will also be diagonal

[1] Note that t has been set to the initial simulation time t_0 without loss of generality.

$\mathbf{\Lambda} = \mathrm{diag}\{\lambda_1, \lambda_2, \ldots, \lambda_N\}$. The elements in the diagonal are called the *characteristic exponents* of the continuous system, and are also the eigenvalues of the system matrix $\mathbf{A}_\mathrm{L}$:

$$\lambda_k = \sigma_k + \mathrm{i}\omega_k = \sigma_k + \mathrm{i}\left(\omega_{p,k} + j_k\Omega\right), \quad j_k \in \mathbb{Z} \tag{15}$$

$$\sigma_k = \frac{1}{T}\ln\left(|\rho_k|\right) \tag{15a}$$

$$\omega_{p,k} = \frac{1}{T}\arg\left(\rho_k\right),\ \omega_{\mathrm{p},k} \in]-\Omega/2; \Omega/2] \tag{15b}$$

where σ_k, ω_k and $\omega_{p,k}$ are the modal damping, modal frequency and principal frequency of mode k, respectively. Since the complex logarithm has an infinite number of branches, the modal frequency ω_k is undetermined within an integer multiple of the rotor speed Ω.

This indeterminacy does not affect the solution given by (10). However, several approaches are present in the literature in order to handle this inherent frequency indeterminacy, that is, the choice of j_k. Stol [9] suggested to solve it to match modal frequencies present in the frequency-response of the system. Skjoldan [11–13] suggested to select the principal solution such that the harmonic components on the ground-fixed degrees of freedom are minimized, this is, defining the modal frequency as the one to which corresponds the most constant mode shape in multiblade or non-transformed inertial coordinates. Bottasso and Cacciola [8] employed the concept of modal participation factors formerly defined by Peters et *al.* [15], where the norm of the individual harmonic components of the periodic mode shape determines the proportion in which that harmonic contributes to the response of each particular mode.

The transient response of the system in physical coordinates corresponding to a sole perturbation of mode k can be expressed as:

$$\mathbf{x}_k(t) = \mathbf{u}_k(t)\mathrm{e}^{\lambda_k(t-t_0)} = \mathbf{u}_k(t)\mathrm{e}^{\left(\lambda_{\mathrm{p},k}+\mathrm{i}j_k\Omega\right)(t-t_0)}, \tag{16}$$

where $\lambda_{p,k} = \sigma_k + \mathrm{i}\omega_{p,k}$ is the principal Floquet exponent of mode k and $\mathbf{u}_k(t)$ the periodic mode shape in physical coordinates, given by

$$\mathbf{u}_k(t) = \boldsymbol{\varphi}(t)\mathbf{v}_k\mathrm{e}^{-\lambda_k(t-t_0)} = \boldsymbol{\varphi}(t)\mathbf{v}_k\mathrm{e}^{-\left(\lambda_{\mathrm{p},k}+\mathrm{i}j_k\Omega\right)(t-t_0)} = \mathbf{u}_{p,k}(t)\mathrm{e}^{-\mathrm{i}j_k\Omega(t-t_0)}. \tag{17}$$

In the above equation, $\mathbf{u}_{p,k}(t) = \boldsymbol{\varphi}(t)\mathbf{v}_k\mathrm{e}^{-\lambda_{\mathrm{p},k}(t-t_0)}$ is the principal periodic kth mode shape, defined so that it does not depend on the integer j_k and $\mathbf{v}_k$ is the kth column of $\mathbf{V}$, the kth eigenvector obtained from Jordan decomposition of matrix $\mathbf{R}$. Since the principal periodic mode shape $\mathbf{u}_{p,k}(t)$ is T-periodic, it contains only harmonics of an integer multiple of Ω and its elements can be expanded into complex Fourier series as:

$$\mathbf{u}_{p,k}(t) = \sum_{n=-\infty}^{\infty} \boldsymbol{\mathcal{U}}_{n,k}\mathrm{e}^{\mathrm{i}n\Omega t} \approx \sum_{n=-N_F}^{N_F} \boldsymbol{\mathcal{U}}_{n,k}\mathrm{e}^{\mathrm{i}n\Omega t}, \tag{18}$$

where $\boldsymbol{\mathcal{U}}_{n,k}$ is the vector containing the N_s Fourier coefficients of the nth harmonic for mode number k and N_F determines the number of Fourier harmonics used in the decomposition. The relative contribution of the nth harmonic to the kth mode can be measured defining its participation factor, $\phi_{n,k}$, as:

$$\phi_{n,k} = \frac{\|\boldsymbol{\mathcal{U}}_{n,k}\|}{\sum_n \|\boldsymbol{\mathcal{U}}_{n,k}\|}. \tag{19}$$

It may be desirable to choose j_k so that the eigenvalues of $\mathbf{R}$ are coincident with or close to those of the averaged, MBC-transformed system matrix. In the case of an internally and

externally isotropic system this can be done exactly by repeating this analysis based on the MBC-transformed principal periodic modal shape $\mathbf{r}_{p,k}(t)$, defined as

$$\mathbf{r}_{p,k}(t) = \mathbf{T}_C^{-1}(t)\mathbf{u}_{p,k}(t). \tag{20}$$

In this case, $\mathbf{r}_{p,k}(t)$ has a single harmonic, and its participation factor is equal to 1. Setting j_k to the corresponding harmonic number leads to the expected eigenvalues and the mode shape of the MBC-transformed system $\mathbf{r}_k(t) = \mathbf{T}_C^{-1}(t)\mathbf{u}_k(t)$ becomes constant. For mildly anisotropic systems, by selecting j_k as the nth harmonic with highest participation factor, the obtained characteristic exponent will be similar to the corresponding eigenvalue of the averaged MBC transformed system matrix and the periodic mode shape will be made as constant as possible. However, for systems with a higher degree of anisotropy a certain mode may not be precisely defined by a single modal frequency.

3. Exponential integrators in multibody dynamics

Exponential integrators have demonstrated interesting properties in the field of multibody dynamics [16]. Based on the linearized system state and input matrices, provided by an aeroelastic code such as OpenFAST, they integrate the system equations. Let the nonlinear system

$$\dot{\mathbf{x}}(t) = \mathbf{f}(\mathbf{x}(t), \mathbf{u}(t)) \tag{21}$$

linearized as

$$\dot{\mathbf{x}}(t) - \dot{\mathbf{x}}^0 = \mathbf{A}(\mathbf{x}^0, \mathbf{u}^0)(\mathbf{x}(t) - \mathbf{x}^0) + \mathbf{B}(\mathbf{x}^0, \mathbf{u}^0)(\mathbf{u}(t) - \mathbf{u}^0), \tag{22}$$

with $\mathbf{A} = \frac{\partial \mathbf{f}}{\partial \mathbf{x}}$ and $\mathbf{B} = \frac{\partial \mathbf{f}}{\partial \mathbf{u}}$. The so-called a *Zero Order Hold* (ZOH) exponential discretization shown in [16] takes the form:

$$\mathbf{x}_{k+1} = \mathbf{x}_k^0 + e^{\mathbf{A}(\mathbf{x}_k^0, \mathbf{u}_k^0)\Delta t}\left(\mathbf{x}_k - \mathbf{x}_k^0\right) + \Delta t \boldsymbol{\varphi}^{\mathbf{1}}(\mathbf{A}(\mathbf{x}_k^0, \mathbf{u}_k^0)\Delta t)(\mathbf{B}(\mathbf{x}_k^0, \mathbf{u}_k^0)\left(\mathbf{u}_k - \mathbf{u}_k^0\right) + \dot{\mathbf{x}}_k^0) \tag{23}$$

where $\mathbf{x}_k$ and $\mathbf{u}_k$ are the system state and input vectors at integration step k. $\dot{\mathbf{x}}^0$, $\mathbf{x}_k^0$ and $\mathbf{u}_k^0$ are the state derivative, state and input vectors at the linearization point, and $\mathbf{A}_k$ and $\mathbf{B}_k$ are the system state and input matrices given by that linearization. A nearby point at the stationary periodic orbit is used at each integration step when determining the *fundamental solution matrix* for Floquet stability analysis. Note that OpenFAST linearization provides all the required information: $\dot{\mathbf{x}}^0$, $\mathbf{x}_k^0$, $\mathbf{u}_k^0$, $\mathbf{A}_k$ and $\mathbf{B}_k$.

Given that the system state and its derivative are known at the linearization points in the stationary periodic orbit, we have devised an exponential method that computes the state variation with respect to a moving point P in this orbit:

$$\mathbf{z}(t) = \mathbf{x}(t) - \mathbf{x}^P(t). \tag{24}$$

We call *along-the-path* or *moving-point exponential integration* (MPEI) to the exponential integration schemes that exploit this idea. In comparison, we call standard exponential integration, as the previous one, *Fixed-Point Exponential Integration* (FPEI). Eq. (22) can be recast to $\dot{\mathbf{z}}(t) = \mathbf{A}\mathbf{z}(t) + \boldsymbol{\upsilon}(t)$, where $\boldsymbol{\upsilon}(t) = \dot{\mathbf{z}}(t) - \mathbf{A}(\mathbf{x}^0, \mathbf{u}^0)\mathbf{z}(t) = \mathbf{B}(\mathbf{x}^0, \mathbf{u}^0)(\mathbf{u}(t) - \mathbf{u}^P(t))$. Then, for a ZOH discretization:

$$\mathbf{z}_{k+1} = e^{\mathbf{A}(\mathbf{x}_k^0, \mathbf{u}_k^0)\Delta t}\mathbf{z}_k + \Delta t \boldsymbol{\varphi}^1(\mathbf{A}(\mathbf{x}_k^0, \mathbf{u}_k^0)\Delta t)\boldsymbol{\upsilon}_k. \tag{25}$$

From (24) the state vector is recovered as $\mathbf{x}_{k+1} - \mathbf{x}_{k+1}^P = \mathbf{z}_{k+1}$, leading to:

$$\mathbf{x}_{k+1} = \mathbf{x}_{k+1}^P + e^{\mathbf{A}(\mathbf{x}^0, \mathbf{u}^0)\Delta t}\mathbf{z}_k + \Delta t \boldsymbol{\varphi}^1(\mathbf{A}(\mathbf{x}_k^0, \mathbf{u}_k^0)\Delta t)\mathbf{B}(\mathbf{x}_k^0, \mathbf{u}_k^0)(\mathbf{u}_k - \mathbf{u}_k^P). \tag{26}$$

In the equations above, Δt denotes the integration time step and $\boldsymbol{\varphi}^1 = (\mathbf{A}\Delta t)^{-1}\left(e^{\mathbf{A}\Delta t} - \mathbf{I}\right)$ is a matrix function that can be numerically computed using diagonal Padé approximants [19].

The filtering effect of the MBC transform can hopefully ease the system integration as in the transformed state the system resembles more closely LTI one [5, 10]. When using a MBC transformed state to integrate based on the previously defined fixed and moving point exponential integrators, we will refer to them as MBC/FPEI and MBC/MPEI respectively. Although the idea presented here can be used with any exponential integrator, its presentation and results in this article are based on the ZOH exponential integrator type [16].

4. Application to wind turbine models

The described exponential integrators have been used in order to test the different integrators and perform Floquet stability analysis for 3-bladed systems with different number of DOFs, as well as a varying degree of anisotropy.

4.1. Simple rotor-drivetrain-tower model (6 DOF)

The 6 DOF system (Fig. 1) models a simple 2D wind turbine consisting of the tower/nacelle structure, the drivetrain, and the 3-bladed rotor. A mass m_N models the nacelle attached to the ground by two spring-damper pairs, (k_H, c_H) and (k_V, c_V) along the side-side x_G and up-down y_G coordinates. The generator rotor, with angular position ψ_G, rotates with constant angular velocity $\dot{\psi}_G = 1$ rad/s. The hub, with inertia moment I_D, is attached to the generator rotor by a torsional spring-damper pair, (k_D, c_D) along θ_D coordinate, modeling drivetrain elasticity. The three blades, indexed with $i = 1, 2, 3$, are attached to the hub at a radius a, by torsional spring dampers, (k_i, c_i) along coordinates ψ_i. They are modeled as point masses at a distance b apart from the attachment point with the hub. Gravity force is considered along negative y-axis direction. The numeric value of the parameters that approximate a generic 10 MW wind turbine model are the ones used by Tcherniak [14] and are shown in Table 1.

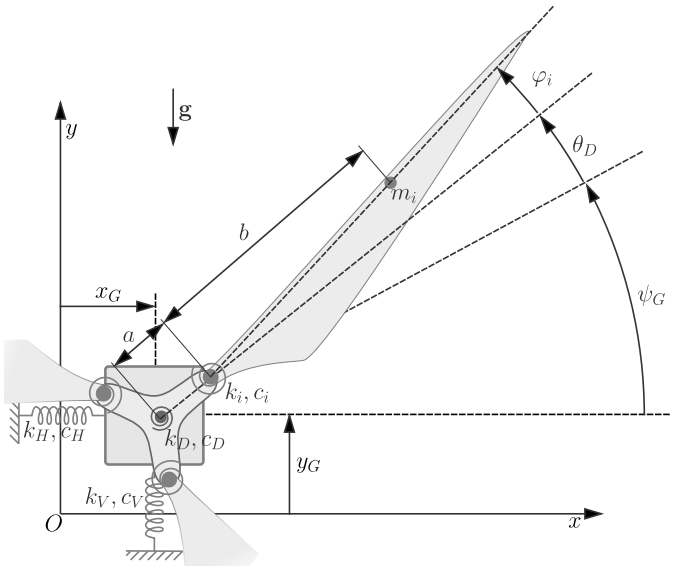

Figure 1. Simplified 6 DOF wind turbine model.

Table 1. Main parameters of the 6 DOF wind turbine model.

Parameter	Symbol	Value	Units
Tower up-down stiffness	k_V	5.2×10^8	N/m
Tower up-down damping	c_V	1.588×10^6	Ns/m
Tower side-side stiffness	k_H	2.6×10^6	N/m
Tower side-side damping	c_H	3.636×10^4	Ns/m
Nacelle mass (including hub)	m_N	4.46×10^5	kg
Drivetrain stiffness	k_D	10^8	N/m
Drivetrain damping	c_D	5.894×10^6	Ns/m
Drivetrain moment of inertia	I_D	2.6×10^7	kgm^2
Blade mass (movable part)	m_i	4.17×10^4	kg
Blade edgewise stiffness	k_i	2.006×10^8	N/m
Blade edgewise damping	c_i	9.813×10^5	Ns/m
Blade hinge offset	a	13.1	m
Distance from hinge to blade CG	b	13.1	m

4.2. Complex aeroelastic model (15 DOF)
The more realistic land-based NREL 5MW reference wind turbine model (NREL 5MW WT) [20] is used. Normal operating conditions are chosen: Rated velocity (12.1 rpm), torque (43.1 kNm) with incoming uniform sheared (0.2 power law exponent) wind of 14 m/s. Collective blade pitch is found to be 6° by prior trim analysis. The 15 enabled DOFs include the tower fore-aft (1st and 2nd assumed modes) and side-side (1st and 2nd modes) bending, drivetrain torsion, blade flapwise (1st and 2nd modes) and edgewise (1st mode) bending and nacelle yaw rotation. Once the steady state is achieved, linearizations are determined using OpenFAST [21] at azimuth steps of 1° in the tower vicinity, to account tower induction, and 5° otherwise.

An additional anisotropic rotor simulation has been performed increasing by 10% the stiffness of one of the blades, while decreasing the stiffness of the remaining blades by 5%.

5. Results and discussion

5.1. Evaluation and comparison of exponential integrators
The proposed exponential integrators are tested for the above models using an initial state deviating from the periodic trajectory. The error w.r.t. the reference integral (MATLAB *ode45* AbsTol= 10^{-14} RelTol= 10^{-14} for the simple rotor, and OpenFAST Adams-Bashforth 4 for NREL 5MW WT), $\varepsilon(t) = \|\mathbf{x}(t) - \mathbf{x}_{ref}(t)\| \, \|\mathbf{x}_{ref}(t)\|^{-1}$, is shown in Fig. 2. For MBC/FPEI and MBC/MPEI state is transformed to non-MBC so that errors are measured on equal basis.

For the simplified rotor model results are shown in Fig. 2a. MPEI and MBC/MPEI integrators show excellent performance, outperforming FPEI and MBC/FPEI, as they show a considerably smaller value and fluctuation. Using MBC is clearly advantageous for FPEI, a bit less for the anisotropic rotor. MPEI and MBC/MPEI performance on par is attributed to the much better performance of MPEI vs FPEI. MBC based integration benefits are questionable in this case.

Higher error values on NREL 5MW WT simulations, are attributed to a higher model complexity. There is a more compelling dynamics due to the tower and wind shear effects and the higher numerical-stiffness of the dynamic model. A smaller performance difference between FPEI and MBC/FPEI integrators is seen, that gets smaller (as expected) for the anisotropic

rotor case (see Fig. 2c), showing somehow bigger error values. This is related to higher variability of system matrix in the anisotropic case. Therefore using MBC for FPEI integration still shows an edge w.r.t. the simple model.

For all the studied systems of different complexity and anisotropy levels, MPEI and MBC/MPEI integrators show outstanding performance and are clearly suitable for Floquet analysis. MBC based integration benefits are questionable for MPEI integrators.

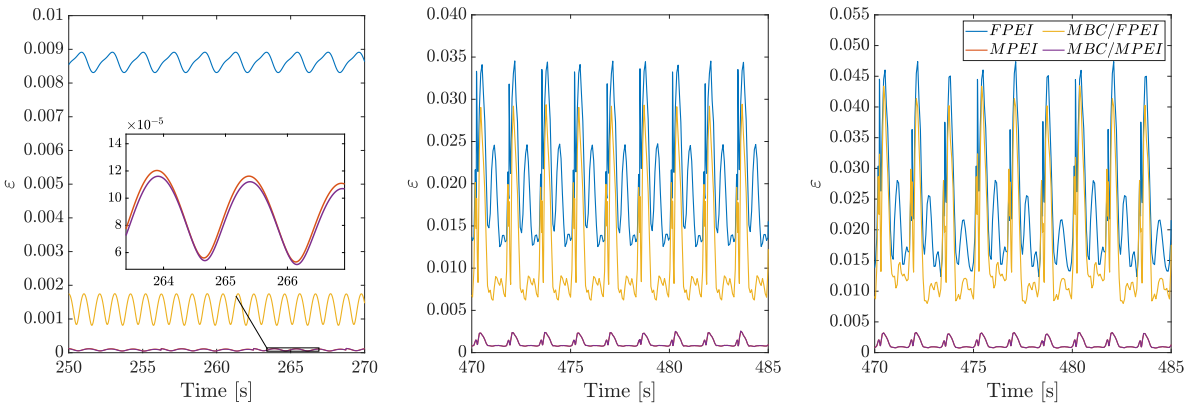

Figure 2. Relative error of different exponential integrators against the reference for the following wind turbine models: (*a*) simple 6 DOF model, (*b*) NREL 5MW WT (isotropic) and (*c*) NREL 5MW WT (anisotropic).

5.2. Floquet stability analysis of the proposed models

The exponential MBC/MPEI has been used in order to perform the Floquet stability analysis for the same cases presented above. Once the stationary periodic trajectory and the linearizations are obtained, the fundamental solution matrix $\boldsymbol{\varphi}(t)$, $t \in [t_0,\ t_0 + T]$ is determined by a set of simulations spanning a single rotation period T starting from initial conditions that separately perturb each state vector component from the initial stationary state. Subsequently, the monodromy matrix $\mathbf{C}$ and its eigenvalues, the Floquet multipliers, are determined. Then, the Floquet factor $\mathbf{R}$ for $j_k = 0$ is calculated and its principal mode shapes expanded into Fourier series. Eigenvalue indeterminacy gets resolved by setting j_k such that its harmonic participation factor, $\phi_{j_k,k}$, is maximum.

The stability results in terms of Floquet multipliers and characteristic exponents for the simple model are shown in Figs. 3a and 3b, respectively. MBC use takes the system very close to LTI, and therefore Floquet and traditional stability approaches give almost identical results. Modal participation factors approach unity for the dominant harmonics in each mode. This result validates our approach and implementation.

As for the isotropic NREL 5MW WT (Figs. 3c and 3d), once again the results do not differ greatly from those obtained with the traditional method. With a maximum of 0.76% deviation in modal damping (real part of the characteristic exponent) between traditional and Floquet approaches. Participation factors are lower than in the previous case with dominant harmonics clearly defined.

More relevant differences are found in modal properties for anisotropic NREL 5MW WT (Figs. 3e and 3f), where larger maximum deviations (8.45%) in modal damping between traditional and Floquet approaches are seen. Indeed, modal participation factors are smaller, with some close to the highest one due to the presence of various harmonics as discussed in [12, 13]. These modes shall not be described by a unique modal frequency, as argued in [8].

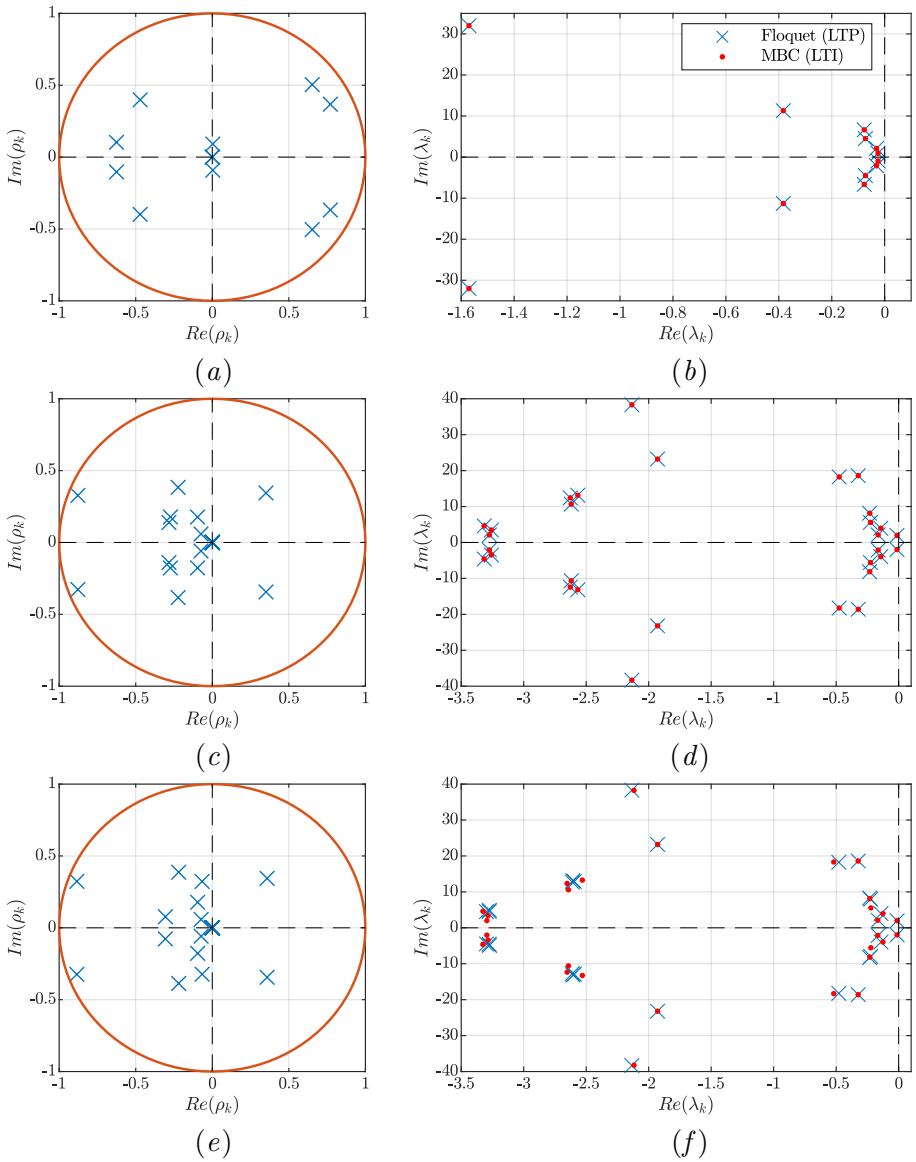

Figure 3. Floquet multipliers (left) and characteristic exponents (right): (a)-(b) simple 6 DOF model, (c)-(d) NREL 5MW WT (isotropic) and (e)-(f) NREL 5MW WT (anisotropic).

6. Conclusions

Exponential integration methods based on system linearizations at several azimuth positions were tested and proposed with focus on Floquet stability analysis of wind turbines. Three different cases of varying complexity and anisotropy levels were analysed. The proposed *along-the-path* or *moving-point* exponential integrator, with or without MBC transformation, was found to be the most suitable one.

The proposed *moving-point* exponential integrator was successfully used for Floquet stability analysis of the three different cases. Quantitative (changes in modal damping) and qualitative (similar modal participation of different harmonics for each mode) differences w.r.t. traditional MBC eigenanalysis were found for the NREL 5MW WT model with an anisotropic rotor. This puts into perspective the relevance of Floquet analysis in wind turbine design.

Acknowledgments
This work has been funded by Gobierno de Navarra's call "Convocatoria 2020 de ayudas a centros tecnológicos y organismos de investigación para la realización de proyectos de I+D colaborativos" under the project PC001-002 AdaptFoil3D II.

References
[1] Holierhoek J G 2020 Aeroelastic Stability Models *Handbook of Wind Energy Aerodynamics* ed B Stoevesandt et al (Springer) ISBN 978-3-030-05455-7
[2] Coleman R P 1943 Theory of self-excited mechanical oscillations of hinged rotor blades Tech. Rep. NACA-WR-L-308. Langley Memorial Aeronautical Laboratory, Langley Field, Va.
[3] Hansen M H 2003 Improved Modal Dynamics of Wind Turbines to Avoid Stall-induced Vibrations *Wind Energy* **6** pp 179–95
[4] Hansen M H 2004 Aeroelastic Stability Analysis of Wind Turbines Using an Eigenvalue Approach *Wind Energy* **7** pp 133–43
[5] Bir G S 2008 Multi-Blade Coordinate Transformation and Its Application to Wind Turbine Analysis *Proc. of the AIAA Wind Energy Symposium, Reno, Nevada*
[6] Bir G S 2010 User's Guide to MBC3: Multi-Blade Coordinate Transformation Code for 3-Bladed Wind Turbines Tech. Rep. NREL/TP-500-44327. Golden, CO: National Renewable Energy Laboratory (NREL)
[7] Jonkman J M and Buhl Jr M L 2005 Fast user's guide Tech. Rep. NREL/TP-500-38230. Golden, CO: National Renewable Energy Laboratory (NREL)
[8] Bottasso C L and Cacciola S 2015 Model-independent periodic stability analysis of wind turbines C.L. *Wind Energy* **18** pp 865–887
[9] Stol K, Balas M and Bir G 2002 Floquet Modal Analysis of a Teetered-Rotor Wind Turbine *J. of Solar Energy Engineering, Trans. of the ASME* **124** pp 364–71
[10] Stol K, Moll H, Bir G and Namik H 2009 A Comparison of Multi-Blade Coordinate Transformation and Direct Periodic Techniques for Wind Turbine Control Design *47th AIAA Aerospace Sciences Meeting, Jan 5-8 2009, Orlando, Florida, AIAA 2009-0439*
[11] Skjoldan P F 2011 *Aeroelastic modal dynamics of wind turbines including anisotropic effects* Ph.D. thesis Danmarks Tekniske Universitet, Risø Nationallaboratoriet for Bæredygtig Energi. Risø-PhD No. 66
[12] Skjoldan P F and Hansen M H 2009 On the similarity of the Coleman and Lyapunov-Floquet transformations for modal analysis of bladed rotor structures *J. of Sound and Vibration* **327** pp 424–39
[13] Skjoldan P F 2009 Modal Dynamics of Wind Turbines with Anisotropic Rotors *Proc. of 47th AIAA Aerospace Sciences Meeting, Orlando, Florida* **327**
[14] Tcherniak D 2015 Rotor anisotropy as a blade damage indicator for wind turbine structural health monitoring systems *Mechanical Systems and Signal Processing* **74** pp 183–198
[15] Peters D A, Lieb S M and Ahaus L A 2011 Interpretation of Floquet Eigenvalues and Eigenvectors for Periodic Systems *J. of the American Helicopter Society* **56**
[16] Ros J, Plaza A, Iriarte X and Ángeles J 2012 Exponential Integration Schemes in Multibody Dynamics *The 2nd Joint International Conf. on Multibody System Dynamics*
[17] Floquet G 1883 Sur les équations différentielles linéaires a coefficients périodiques *Annales scientifiques de l'É.N.S. 2e série* (12) pp 47–88
[18] Lyapunov A M 1992 *General Problem of the Stability Of Motion* (London: Taylor and Francis) ISBN 0748400621
[19] Berland H, Skaflestad B and Wright W M 2007 Expint—a matlab package for exponential integrators *ACM Trans. Math. Softw.* **33** 4–es
[20] Jonkman J M, Butterfield S, Musial W and Scott G 2007 Definition of a 5-mw reference wind turbine for offshore system development Tech. Rep. NREL/TP-500-38060. Golden, CO: National Renewable Energy Laboratory (NREL)
[21] Jonkman J M and Jonkman B J 2016 FAST modularization framework for wind turbine simulation: full-system linearization *J. of Physics: Conference Series* **753**